Chemical Engineering Journal 435 (2022) 134854

Contents lists available at ScienceDirect

Chemical Engineering Journal

journal homepage: www.elsevier.com/locate/cej

Short communication

Are microbubbles magic or just small? a direct comparison of hydroxyl radical generation between microbubble and conventional bubble ozonation under typical operational conditions

Alexander John [a], Irene Carra [a], Bruce Jefferson [a], Monika Jodkowska [a], Adam Brookes [b], Peter Jarvis [a,*]

[a] Cranfield Water Science Institute, Cranfield, UK
[b] Anglian Water, Thorpe Wood House, Peterborough, UK

ARTICLE INFO

Keywords:
Microbubbles
Ozone
Hydroxyl radicals
Water treatment

ABSTRACT

The application of microbubbles for water treatment is an emerging technology which has been shown to significantly enhance gas–liquid contacting processes. When applied to ozonation, microbubble technology has been shown to enhance mass transfer and the speed and extent of compound removal compared with conventional bubbling techniques. One explanation as to why microbubble systems outperform conventional systems is that microbubbles shrink, collapse and spontaneously generate hydroxyl radicals which is thought to enhance the speed of compound removal. This study compared microbubble (mean diameter 37 μm) and conventional bubble (mean diameter 5.4 mm) ozonation systems under identical conditions. The experiments were normalised for effective ozone dose to determine whether microbubble ozonation generated significantly more hydroxyl radicals than conventional bubble ozonation. 4-chlorobenzoic was used as the hydroxyl radical probe and the proportion of hydroxyl radicals generated for a given effective ozone dose was quantified. The $^{\bullet}$OH-exposure to O_3-exposure (the R_{ct}) was used to compare the systems. The ratio of the mean $R_{ct(Microbubble)}$ to mean $R_{ct(Conventional)}$ was 0.73, 0.84 and 1.12 at pH 6, 7 and 8 respectively. Statistical assessment of the R_{ct} showed that there was no significant difference between the bubble systems. No evidence was found to support the hypothesis that microbubble systems generate more $^{\bullet}$OH. Instead, the level of $^{\bullet}$OH-exposure is linked to the effective dose and pH of the system and future designs should focus on those factors to deliver $^{\bullet}$OH based benefits.

1. Introduction

Recent technology advances have enabled the generation of microbubbles (1 – 100 μm) to become more widely applicable for use in drinking water treatment beyond dissolved air flotation. Previous research has shown that the use of microbubbles in place of conventionally produced fine bubbles can enhance mass transfer [25], increase gas utilisation efficiency [38] and increase the rate and extent of compound removal [2] during ozonation. As such, they are now being considered to replace conventional bubble (2 – 6 mm) systems [9].

The observed performance enhancement is commonly attributed to the large size difference between microbubbles and conventional bubbles [30]. This size difference results in a significantly higher interfacial area [22] and a decrease in rise velocity leading to an extended contact time for the microbubble systems compared to conventional systems [24]. These features allow for a faster and more extensive transfer of gas into the liquid phase [27] which can lead to enhanced treatment [9].

When ozone is dissolved in water it undergoes a series of pH dependent, complex self-decomposition reactions that lead, in part, to the formation of desirable hydroxyl radicals ($^{\bullet}$OH). $^{\bullet}$OH are highly oxidising and non-selective and have been shown to be beneficial to the degradation of recalcitrant compounds [9]. A number of recent papers have proposed enhanced $^{\bullet}$OH generation from microbubbles as an additional benefit [11,15,18,25,31,23,39]. One proposed mechanism for this being that microbubbles shrink and collapse; rapidly causing an extreme internal temperature and pressure that results in $^{\bullet}$OH generation. This mechanism has been evidenced in bubble cavitation with a dynamic stimulus such as ultrasound (Thanh Nguyen et al., 2017; [20]. However, many authors studying application of microbubbles report that their collapse and subsequent production of $^{\bullet}$OH contributes to

* Corresponding Author.
E-mail address: p.jarvis@cranfield.ac.uk (P. Jarvis).

https://doi.org/10.1016/j.cej.2022.134854
Received 29 October 2021; Received in revised form 10 January 2022; Accepted 19 January 2022
Available online 24 January 2022

enhanced performance without any such stimulus (Table 1). This has been reported for microbubbles that cover a size range from 1 to 450 μm. It is also the case that many microbubble studies provide limited information on bubble physical characteristics and hence do not always report a size or compare performance directly with conventional bubbles.

It therefore remains equivocal as to whether microbubbles offer an enhanced generation of •OH over conventional systems as researchers have reported that microbubbles cannot shrink and collapse fast enough to generate •OH spontaneously [28,1,37]. The aim of the current work was to test the hypothesis that microbubbles generate an enhanced concentration of •OH compared to conventionally sized bubbles under conditions that were representative of typical operating conditions for ozone systems used in water treatment. To test this a set of controlled experiments directly comparing •OH generation from microbubble and conventional bubbles were trialled in the same setup at three pH's which are most representative of operational ozonation pH's (6, 7, 8). The majority of research on microbubble ozonation is conducted in relatively short column (<1 m) laboratory trails at fixed ozone input doses which generates a positive bias toward microbubble systems [9]. The faster mass transfer associated with microbubble ozonation generates near complete transfer of the available ozone within 1 m and hence delivers a higher dissolved ozone concentration, generating a proportional increase in absolute •OH concentration. However, this does not translate to full scale systems where greater water depths are used (3 – 7 m) resulting in less difference in overall transfer [9]. To obviate such bias the microbubble and conventional bubble systems were operated to achieve equivalent effective dissolved ozone concentrations and thus enable direct observation of any differential •OH generation. This is rarely, if ever, done in previous studies when different sized bubbles have been compared. As such, a sub-hypothesis that the O_3-exposure was different between the microbubble and conventional bubble systems at a fixed effective dose was tested.

2. Materials and methods

2.1. Materials

4-chlorobenzoic acid (pCBA) (≥99 %, Sigma Aldrich) was used as the •OH probe. Sodium hydroxide (NaOH, Technical Grade, Fisher) and sulphuric acid (H_2SO_4, Technical Grade, Fisher) were used as pH modifiers. N,N-diethyl-1,4-phenylene diamine (DPD) photometric O_3 tests (Merck) were used to measured dissolved O_3 concentration. Potassium iodide (≥98 %, Merck) was used as the quenching agent. Methanol (Liquid chromatography mass spectrometry (LCMS) grade, ≥ 99.9 %, Fisher) and ultrapure water (18 MΩ, Elga Purelab) were used as mobile

Table 1
Current perspective on •OH generation from microbubbles.

Microbubble Diameter / μm	Conventional Bubble Diameter / μm	Normalised For	Position on additional •OH generation	Column Height / m	Author
10–50	1–2	Input dose	Additional •OH could be generated through the shrink and collapse of microbubbles.	Not stated	Jothinathan et al. [11]
10.30 – 10.60	Not tested	No comparison with conventional	Due to pyrolytic decomposition that takes place within collapsing bubbles, •OH can be generated at the gas–liquid interface.	Not stated	Wan et al. [31]
0.22–50	0.5–1	Input dose	The constant shrink and collapse of microbubbles result in a powerful pressure wave and high mechanical shear force which further eliminates pollutants.	0.7	Sun et al. [25]
Not stated	Not stated	Input dose	Shrink and collapse of microbubbles will generate numerous hydroxyl radicals.	Conventional: 0.6Microbubble: 0.3	Liu et al. [18]
Not stated	Not tested	No comparison with conventional	By gradually shrinking in size, microbubbles break up in the liquid phase and produce •OH.	Not stated	Li et al. [15]
44–450	Not tested	No comparison with conventional	•OH can be generated due to the pyrolytic decomposition of ozone within the collapsing microbubbles.	Not stated	Patel et al. [23]
5 – 25 μm	Not stated	Input dose	The increased concentration of •OH in the aqueous phase by collapsing O_3 microbubbles may contribute to the removal of trace organic compounds.	Not stated	Lee et al. [14]
Not stated	Not stated	Input dose	The collapse of microbubbles produces •OH which are associated with ion packing around the collapsed microbubbles.	0.9	Huang et al. (2019)
2.35 ± 0.84	Near 3	Input dose	Microbubble collapse can generate a shock wave that generates free radicals.	Not stated	Gao et al. [6]
Not stated	Not stated	Input dose	When ozone microbubbles shrink it has been reported that they will burst instantaneously and generate •OH.	Not stated	Cheng et al. [4]
20–50	Not stated	Input dose	Higher ozone self-decomposition in microbubble systems might result from the shrink and collapse.	Conventional: 0.6Microbubble: 0.3	Wu et al. [34]
51.4	Not stated	Input dose	Microbubbles shrink and collapse in the liquid phase and •OH could be generated. •OH generated from collapsing microbubbles probably promote chain reactions of O_3 decomposition.	0.5	Zhang et al. [38]
10–50	Not stated	Input dose	Free radicals might be generated when microbubbles collapse.	Not stated	Li et al. [17]
0.247 ± 0.009	Not stated	Input dose	No evidence of free radical production from air microbubbles.	0.76	Hu and Xia [8]
Not stated	Not stated	Input dose	More generation of •OH might be another cause for the increasing rate of reaction in microbubble ozonation.	0.5	Wang et al. [32]
0.06 – 0.150 and 50	Not tested	No comparison with conventional	At pH ≤ 3, collapsed microbubbles could generate hydroxyl radicals.	Not stated	Sung et al. [26]
2.6	Not stated	Input dose	•OH generation from collapsing microbubbles during ozonation contributed to the degradation of wastewater.	0.25 rising distance	Yao et al. [36]
65 % of bubbles had a diameter < 30	Not tested	No comparison with conventional	•OH are very effectively generated by the collapse of O_3 microbubbles in aqueous solutions.	Not stated	Jabesa and Ghosh [10]
< 45	Approximately 1	Input dose	The enhanced performance could be ascribed to greater amounts of •OH being generated during the collapse of O_3 microbubbles as well as the self-decomposition of O_3 at pH 8.	1.2	Zheng et al. [39]

phases for LCMS analysis. Ammonium acetate (≥98 %, Sigma Aldrich) was used as a buffer for the mobile phases. Deionised water (15 MΩ, Elga Purelab) was used as the aqueous medium for the experiments.

2.2. Experimental setup

Semi-batch microbubble and conventional bubble experiments were performed in a cylindrical acrylic reactor (Model Products) with a height of 80 cm and a diameter of 45 cm. The experiments were conducted in 100 L of deionised water with a water height of 67 cm.

O_3 was generated from compressed air using a corona discharge O_3 generator (C-Lasky C-L010-DT, Advanced Ozone Products) with an O_3 production of up to 2 g h^{-1} and an operational gas flow rate range of 2 – 10 L min^{-1} at atmospheric pressure. The gas flow rate was set to 2 L min^{-1} for all experiments. Microbubbles with a Sauter mean diameter (d_{32}) of 37 μm (Fig. 2) were generated using a regenerative turbine microbubble generator (Nikuni KTM20N trial unit, Aeration & Mixing). The microbubble generator had a recirculating liquid flow rate of 16.6 L min^{-1} and a gas flow rate with a range of 0 – 5 L min^{-1}. The gas flow intake of the microbubble generator was set to 2 L min^{-1} for all experiments. The aqueous phase was continuously recirculated through the microbubble generator. Conventional bubbles with a d_{32} of 5.4 mm (Fig. 2) were generated from a fine pore diffuser (132 mm ceramic air stone diffuser, Finest Aquatic LTD) connected directly to the O_3 generator. From the gas flow and bubble size distribution data, the quantity of bubbles generated was calculated to be 7.54×10^{10} bubbles min^{-1} for the microbubble system and 2.4×10^4 bubbles min^{-1} for the conventional system. This equated to a bubble density of 3.77×10^{10} and 1.2×10^4 bubbles L^{-1} for the microbubble and conventional systems respectively. A separate pump (AF-1500, Hidom) recirculated the aqueous phase with a flow rate of 16.6 L min^{-1}. pH was measured using a portable pH meter (HI-8424, Hanna Instruments), water resistant pH electrode (HI-1230B, Hanna Instruments) and temperature probe (HI-7662, Hanna Instruments). pH was modified using sodium hydroxide or sulfuric acid. The pH was maintained ± 0.1 throughout each experiment with dropwise addition of dilute sodium hydroxide or sulfuric acid without the presence of buffer. The aqueous temperature for all experiments was 20 ± 1 ℃ (Fig. 1).

The experiments were set for a fixed effective ozone dose of 2.75 μmol L^{-1} min^{-1} to avoid any experimental bias. The ozone output power was set to 100% for the conventional bubble experiments. This equated to 130 W of O_3 output. In order to achieve an equivalent fixed effective O_3 dose for the microbubble system, the ozone output power was reduced to 75 W for the microbubble ozonation experiments. This accounted for the increased gas utilisation efficiency of the microbubble system and allowed for equivalent O_3-exposures for both systems.

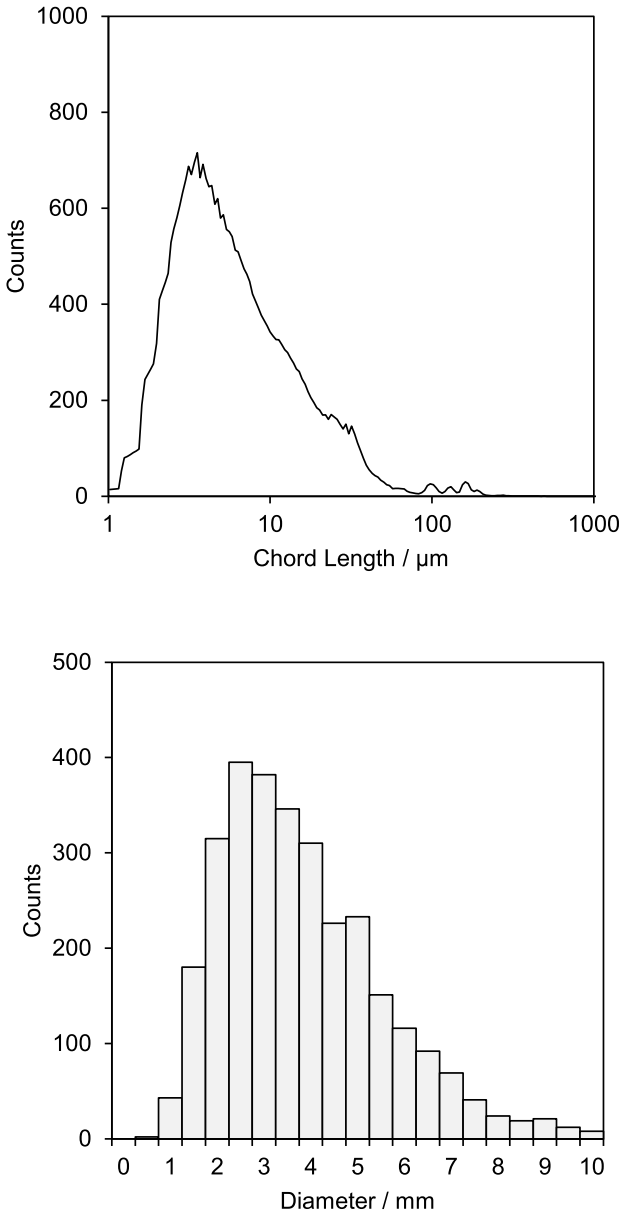

Fig. 2. Size distributions of microbubbles (top) and conventional bubbles (bottom).

2.3. Analysis method

The •OH concentration was measured with an indirect method using pCBA as a probe compound as previously developed [5] to overcome issues associated with the highly reactive and short-lived nature of •OH [12]. The probe compound enables differential measurement of •OH over O_3 as their relative rate constants are significantly different (5.0×10^9 M^{-1} s^{-1} and 0.15 M^{-1} s^{-1} for •OH over O_3 respectively; [35] such that the removal of pCBA can be solely attributed to •OH.

An initial concentration of pCBA of 0.056 μmol L^{-1} was used throughout. At each time interval, 20 mL of sample was withdrawn and immediately quenched with 0.2 mL potassium iodide solution to prevent

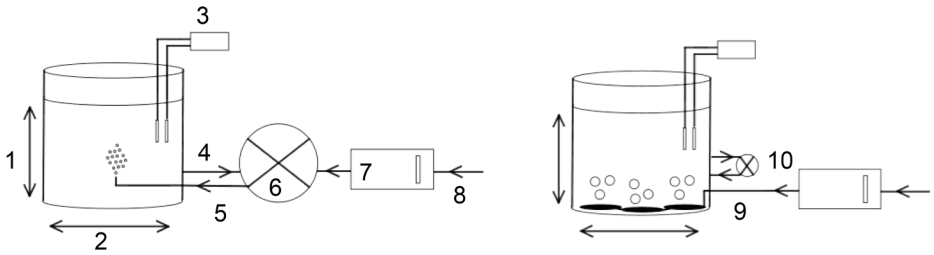

Fig. 1. Experimental setup. Where (1) 0.67 m water height (2) 0.45 m diameter (3) pH and temperature probes (4) water recirculation (5) microbubble input (6) microbubble generator (7) ozone generator (8) gas supply (9) gas supply to diffusers (10) recirculation pump.

further ozonation [3]. 10 mL of sample was then used for dissolved O_3 measurement with the diethyl-p-phenylene diamene (DPD) O_3 test and measured using a photometer (Pharo 300, Spectroquant). The remaining 10 mL was passed through a 0.2 μm filter (Minisart, Sartorius) for LCMS analysis. pCBA concentration was determined using LCMS (ExionLC, Triple Quad 5500+, Sciex). An Acquity C18 ethylene bridged hybrid column (1.7 μm × 2.1 mm × 50 mm) (Waters) maintained at 40 ℃ was used and the sample injection volume was 5 μL. The mobile phase flow rate was 0.45 mL min^{-1}. The mobile phase consisted of ultrapure water with 2 mMol ammonium acetate (A) and methanol with 2 mMol ammonium acetate (B). The initial mobile phase ratio was 90: 10 A:B and ramped linearly to 5:95 A:B over 4 min before returning to 90:10 A:B for the final minute for a total run time of 5 min per sample. The limit of detection and limit of quantification were 0.11 and 0.33 μg L^{-1} respectively.

Bubble size was measured using focus-beam reflectance measurement (FBRM D600L, Mettler Toledo) for the microbubble system. For the conventional system, high speed video was captured (HERO8, GoPro), video frames were extracted (VLC Media Player, VideoLAN) and processed with image processing software (ImageJ).

The integrated form of the rate equation shows that pCBA removal is related to the time-integral of •OH concentration; known as •OH-exposure [5] (Equation (1)):

$$ln\left(\frac{[pCBA]}{[pCBA]_0}\right) = -k_{\cdot OH(pCBA)}\int[\cdot OH]dt \quad (1)$$

Where $[pCBA]$ is pCBA concentration (mol L^{-1}), $[pCBA]_0$ is the initial pCBA concentration (mol L^{-1}), $k_{\cdot OH(pCBA)}$ is the rate constant for the reaction of pCBA with •OH (L mol^{-1} s^{-1}) and $\int[\cdot OH]dt$ is the time integral of [•OH] (mol L^{-1} s). Therefore, the removal of pCBA over time is an indirect measurement of •OH generation.

To test the main hypothesis, the ratio of •OH measured to O_3 dose delivered was compared (Equation (2)):

$$R_{ct} = \frac{\int[\cdot OH]dt}{\int[O_3]dt} \quad (2)$$

Where $\int[O_3]dt$ is the time-integrated dissolved O_3 concentration (mol L^{-1} s) and R_{ct} is the ratio of •OH-exposure to O_3-exposure. R_{ct} can be calculated from a graphical plot of the change in pCBA concentration over time against the time-integrated dissolved O_3 concentration (Equation (3)):

$$ln\left(\frac{[pCBA]}{[pCBA]_0}\right) = -k_{\cdot OH(pCBA)}R_{ct}\int[O_3]dt \quad (3)$$

3. Results and discussion

The pseudo-first order rate constant for the removal of pCBA ($k_{\cdot OH(pCBA)}$) increased as pH increased for both the microbubble and conventional bubble systems (Supplementary Figure 1). To illustrate, at pH 6, 7 and 8 the value of $k_{\cdot OH(pCBA)}$ was 0.07 ± 0.004, 0.48 ± 0.09 and 0.86 ± 0.07 min^{-1} for the microbubble system and 0.09 ± 0.01, 0.57 ± 0.1 and 0.97 ± 0.09 min^{-1} for the conventional bubble system. If the main hypothesis was true then $R_{ct(Microbubble)}$ would be greater than $R_{ct(Conventional)}$ due to enhanced •OH generation related to microbubble collapse. This was tested at three different pH levels to reflect changes in the O_3-exposure which decreased with increasing pH due to the associated change in the rate of O_3 self-decomposition (Supplementary Figure 2). After 10 min of ozonation, the O_3-exposure for the microbubble system was 173.8 ± 11.8, 133.5 ± 11.7 and 102.3 ± 4.9 μmol L^{-1} min at pH 6, 7 and 8 respectively. The comparative data for the conventional bubble system was 194.4 ± 21.6, 154.5 ± 7.5 and 116.0 ± 14.8 μmol L^{-1} min. The difference in O_3-exposure between the two bubble systems at each pH was not significantly different based on a two-tailed Mann-Whitney U test with a confidence interval of 95 %. The p-values at pH 6, 7 and 8 were 0.40, 0.10 and 0.38 such that the sub-hypothesis that the O_3-exposures were different between microbubble and conventional bubble systems (h_1) was rejected and hence any difference in •OH concentration could be associated with enhanced generation.

The R_{ct} was calculated from the change in pCBA concentration over time against the time-integrated dissolved O_3 concentration (Fig. 3). For microbubble ozonation, R_{ct} values of 1.77 × 10^{-8} ± 3.91, 2.17 × 10^{-7} ± 4.98 × 10^{-8} and 4.79 × 10^{-7} ± 7.12 × 10^{-8} were obtained at pH 6, 7 and 8 respectively. In comparison, the equivalent R_{ct} values for the conventional bubble system were 2.40 × 10^{-8} ± 4.49 × 10^{-9}, 2.59 × 10^{-7} ± 3.39 × 10^{-8} and 4.27 × 10^{-7} ± 9.37 × 10^{-8} at pH 6, 7 and 8 respectively. Consequently, the ratio of mean $R_{ct(Microbubble)}$ to mean $R_{ct(Conventional)}$ was 0.73, 0.84 and 1.12 at pH 6, 7 and 8 respectively. Statistical assessment of the R_{ct} value indicated no significant difference could be observed based on the Mann-Whitney U test at a 95 % confidence interval. The p-values obtained were 0.16, 0.51 and 1.0 for the comparison of microbubble and conventional bubble R_{ct} values at pH 6, 7 and 8 respectively. Since $p > 0.05$ for all comparison, h_1 was rejected and hence the R_{ct} values for each comparison were the same.

The impact of R_{ct} and O_3-exposure data on the resultant •OH-exposures revealed an increase as a function of pH with the biggest change occurring as the water increased from slightly acidic to neutral (Fig. 4). To illustrate, •OH-exposure was 3.1 × 10^{-12} ± 1.8 × 10^{-13} mol L^{-1} min for the microbubble system and 4.6 × 10^{-12} ± 0.6 × 10^{-12} mol L^{-1} min for the conventional system at pH 6. In the case of the conventional bubble systems, this increased to 3.9 × 10^{-11} ± 4.5 × 10^{-12} mol L^{-1} min and 4.8 × 10^{-11} ± 1.0 × 10^{-11} mol L^{-1} min for pH 7 and 8 respectively. The corresponding data for the microbubble system was 3.2 × 10^{-11} ± 9.0 × 10^{-12} and 4.1 × 10^{-11} ± 5.7 × 10^{-12} mol L^{-1} min. This represented an increase in mean values of 10.2 times and 13.2 times compared to pH 6 for the microbubble system and 8.4 and 10.4 times for the conventional bubble system. Overall, this confirms the benefit of operating away from slightly acidic conditions when wanting to maximise •OH-exposure. •OH production from ozonation is generally accepted to proceed solely through O_3 self-decomposition [7]. O_3 self-decomposition is not fully understood, however there are two generally accepted self-decomposition pathways [9]. Both of these reaction routes are initiated by the hydroxide ion and, as such, these results lend support to the notion that •OH production is primarily a consequence of the speed of O_3 self-decomposition. This implies that as the pH increased, the speed of O_3 self-decomposition increased as the concentration of hydroxide ions increased. This culminated in the expected observation that as pH increased, •OH production increased and thus •OH-exposure also increased.

Overall, statistical testing of the data with a Mann-Whitney U test ($p < 0.05$) showed no significant difference in •OH generation between microbubble and conventional systems and so the hypothesis can be rejected. The Mann-Whitney U test was used in order to assess whether the difference in observed $\int$[•OH]dt values between the microbubble system and conventional bubble system were statistically significant. It was found that, at the 95 % confidence level, the hypothesis that either microbubble or conventional bubble ozonation produced a higher proportion of •OH for a given O_3 dose cannot be accepted at any of the tested pH's and it must be assumed that the $\int$[•OH]dt values are equal.

A large proportion of the microbubble-ozonation literature suggests that •OH generated from collapsing microbubbles is an important component in enhancing the performance of microbubble systems. The current research has shown this is not an important mechanism under normal operational conditions for ozone treatment (pH 6–8). Some researchers have reported spontaneous •OH generation from collapsing microbubbles but only under specific, strongly acidic conditions for which the mechanism is not fully understood [28,16,13,21]. However, these researchers did not observe •OH generation at slightly acidic, neutral or alkaline pH. It is not fully been fully explained as to why

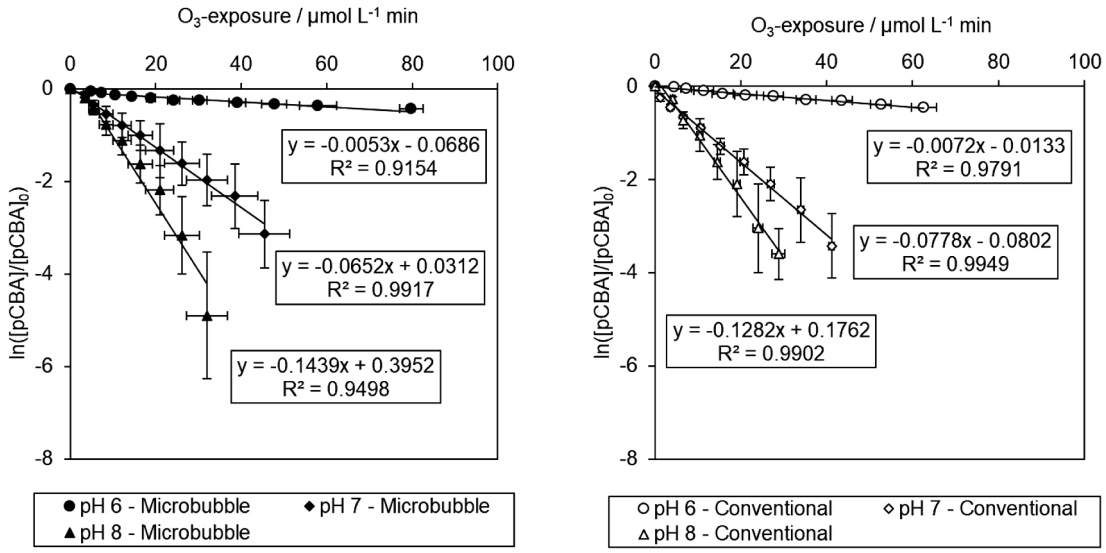

Fig. 3. Plots of $ln\left(\frac{[pCBA]}{[pCBA]_0}\right)$ vs. $\int[O_3]dt$ at pH 6, 7 and 8 for microbubble (top) and conventional bubble (bottom) ozonation of pCBA.

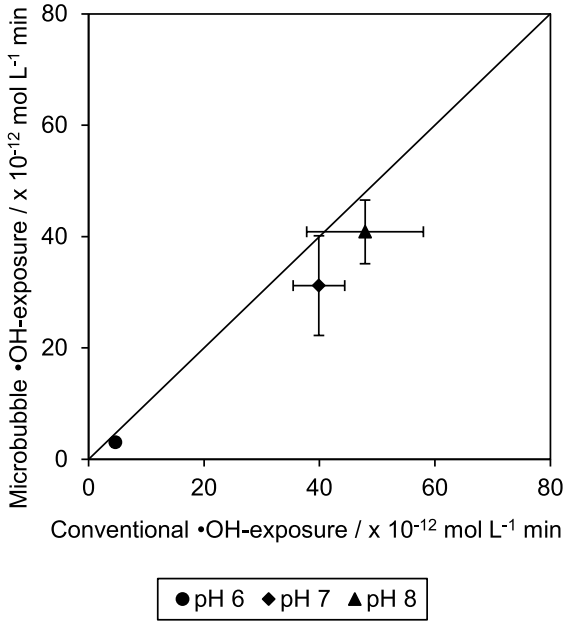

Fig. 4. Parity plot of $\int$[•OH]dt for microbubble vs. conventional bubble ozonation at pH 6, 7 and 8.

strongly acidic conditions are required, however it has been proposed that the addition of strong acid causes a change in the electrical properties of the gas–liquid interface which does not occur under slightly acidic, neutral or alkaline conditions. Additional •OH generation from collapsing microbubbles under neutral or alkaline conditions has not been observed in other studies [8]. Even when nanobubbles as small as 40 nm have been used, under normal operational pH conditions no •OH was detected and the addition of strong acid was required to trigger •OH generation [29]. Spontaneous production of •OH from bubble collapse is only expected to be seen for bubbles in the low nm diameter size range [19] or where the is the presence of acoustic stimuli, such as ultrasound [33].

These results support the view that the quantity of •OH produced is proportional to the effective O_3 dose and that any reported enhancement of •OH when using microbubbles is explained by that. Accordingly, the greater O_3 mass transfers afforded in the laboratory set ups for microbubble systems generates an artefact that may not translate into full scale practice where overall gas utilisation efficiencies will be more closely matched. However, the ability to transfer high doses into small volumes of water through microbubble systems offers the possibility of alternative designs that benefit from such outcomes and where the dose related enrichment of •OH could be positively utilised.

4. Conclusion

The presented data has provided evidence to show that the amount of •OH produced through microbubble and conventional bubble ozonation are the same for equivalent O_3-exposure. This study has not found evidence to support the view that microbubble ozonation produces more •OH than conventional bubble ozonation when effective O_3 doses are equivalent. The evidence presented here implies that the collapse of microbubbles does not cause the spontaneous generation of •OH under the tested conditions within a typical operational pH range of 6 – 8 for most ozone applications in water treatment. This study supports the notion that •OH production is directly linked to the O_3 self-decomposition pathway and that other mechanisms for •OH production such as microbubble collapse are either negligible or not present under the pH conditions tested and for the prevailing bubble size distribution.

Declaration of Competing Interest

The authors declare that they have no known competing financial interests or personal relationships that could have appeared to influence the work reported in this paper.

Acknowledgements

This research is gratefully supported by the Engineering and Physical Sciences Research Council (EPSRC) through their funding of the STREAM Industrial Doctorate Centre (EP/ G037094/1) and from the project sponsor Anglian Water.

Appendix A. Supplementary data

Supplementary data to this article can be found online at https://doi.org/10.1016/j.cej.2022.134854.

References

[1] A. Agarwal, W.J. Ng, Y.u. Liu, Principle and applications of microbubble and nanobubble technology for water treatment, Chemosphere 84 (9) (2011) 1175–1180.

[2] T. Azuma, K. Otomo, M. Kunitou, M. Shimizu, K. Hosomaru, S. Mikata, Y. Mino, T. Hayashi, Removal of pharmaceuticals in water by introduction of ozonated microbubbles, Separation and Purification Technology 212 (2019) 483–489.

[3] H. Bader, J. Hoigné, Determination of ozone in water by the indigo method, Water Research 15 (4) (1981) 449–456.

[4] W. Cheng, L. Jiang, X. Quan, C. Cheng, X. Huang, Z. Cheng, L. Yang, Ozonation process intensification of p-nitrophenol by in situ separation of hydroxyl radical scavengers and microbubbles, Water Science and Technology 80 (1) (2019) 25–36.

[5] M.S. Elovitz, U. von Gunten, Hydroxyl Radical/Ozone Ratios During Ozonation Processes. I. The R_{ct} Concept, Ozone: Science & Engineering 21 (3) (1999) 239–260.

[6] Y. Gao, Y. Duan, W. Fan, T. Guo, M. Huo, W.u. Yang, S. Zhu, W. An, Intensifying ozonation treatment of municipal secondary effluent using a combination of microbubbles and ultraviolet irradiation, Environmental Science and Pollution Research 26 (21) (2019) 21915–21924.

[7] D. Gardoni, A. Vailati, R. Canziani, Decay of Ozone in Water: A Review, Ozone: Science & Engineering 34 (4) (2012) 233–242.

[8] L. Hu, Z. Xia, Application of ozone micro-nano-bubbles to groundwater remediation, Journal of Hazardous Materials 342 (2018) 446–453.

[9] A. John, A. Brookes, I. Carra, B. Jefferson, P. Jarvis, Microbubbles and their application to ozonation in water treatment: A critical review exploring their benefit and future application, Critical Reviews in Environmental Science and Technology (2020) 1–43.

[10] A. Jabesa, P. Ghosh, Removal of diethyl phthalate from water by ozone microbubbles in a pilot plant, Journal of Environmental Management 180 (2016) 476–484.

[11] L. Jothinathan, Q.Q. Cai, S.L. Ong, J.Y. Hu, Organics removal in high strength petrochemical wastewater with combined microbubble-catalytic ozonation process, Chemosphere 263 (2021) 127980, https://doi.org/10.1016/j.chemosphere.2020.127980.

[12] S. Khuntia, S.K. Majumder, P. Ghosh, Quantitative prediction of generation of hydroxyl radicals from ozone microbubbles, Chemical Engineering Research and Design 98 (2015) 231–239.

[13] S. Khuntia, S.K. Majumder, P. Ghosh, Catalytic ozonation of dye in a microbubble system: Hydroxyl radical contribution and effect of salt, Journal of Environmental Chemical Engineering 4 (2) (2016) 2250–2258.

[14] Y. Lee, Y. Park, G. Lee, Y. Kim, K. Chon, Enhanced Degradation of Pharmaceutical Compounds by a Microbubble Ozonation Process: Effects of Temperature, pH, and Humic Acids, Energies 12 (22) (2019) 4373.

[15] C. Li, S. Yuan, F. Jiang, Y. Xie, Y. Guo, H. Yu, Y. Cheng, H.e. Qian, W. Yao, Degradation of fluopyram in water under ozone enhanced microbubbles: Kinetics, degradation products, reaction mechanism, and toxicity evaluation, Chemosphere 258 (2020) 127216, https://doi.org/10.1016/j.chemosphere.2020.127216.

[16] P. Li, M. Takahashi, K. Chiba, Degradation of phenol by the collapse of microbubbles, Chemosphere 75 (10) (2009) 1371–1375.

[17] P. Li, C. Wu, Y. Yang, Y. Wang, S. Yu, S. Xia, W. Chu, Effects of microbubble ozonation on the formation of disinfection by-products in bromide-containing water from Tai Lake, Separation and Purification Technology 193 (2018) 408–414.

[18] Y. Liu, S. Wang, L. Shi, W. Lu, P. Li, Enhanced degradation of atrazine by microbubble ozonation, Environmental Science: Water Research & Technology 6 (6) (2020) 1681–1687.

[19] S. Liu, S. Oshita, S. Kawabata, Y. Makino, T. Yoshimoto, Identification of ROS produced by nanobubbles and their positive and negative effects on vegetable seed germination, Langmuir 32 (43) (2016) 11295–11302.

[20] N. Masuda, A. Maruyama, T. Eguchi, T. Hirakawa, Y. Murakami, Influence of Microbubbles on Free Radical Generation by Ultrasound in Aqueous Solution: Dependence of Ultrasound Frequency, The Journal of Physical Chemistry B 119 (40) (2015) 12887–12893.

[21] C. Minamoto, N. Fujiwara, Y. Shigekawa, K. Tada, J. Yano, T. Yokoyama, Y. Minamoto, S. Nakayama, Effect of acidic conditions on decomposition of methylene blue in aqueous solution by air microbubbles, Chemosphere 263 (2021) 128141, https://doi.org/10.1016/j.chemosphere.2020.128141.

[22] R. Parmar, S.K. Majumder, Microbubble generation and microbubble-aided transport process intensification—A state-of-the-art report, Chemical Engineering and Processing: Process Intensification 64 (2013) 79–97.

[23] S. Patel, S.K. Majumder, P. Das, P. Ghosh, Ozone microbubble-aided intensification of degradation of naproxen in a plant prototype, Journal of Environmental Chemical Engineering 7 (3) (2019) 103102, https://doi.org/10.1016/j.jece.2019.103102.

[24] Y. Shangguan, S. Yu, C. Gong, Y. Wang, W. Yang, L.-a. Hou, A Review of Microbubble and its Applications in Ozonation, IOP Conference Series: Earth and Environmental Science 128 (2018) 012149, https://doi.org/10.1088/1755-1315/128/1/012149.

[25] Z. Sun, X. Chen, K. Yang, N. Zhu, Z. Lou, The progressive steps for TPH stripping and the decomposition of oil refinery sludge using microbubble ozonation, Science of The Total Environment 712 (2020) 135631, https://doi.org/10.1016/j.scitotenv.2019.135631.

[26] M. Sung, C.-H. Teng, T.-H. Yang, Dissolution enhancement and mathematical modeling of removal of residual trichloroethene in sands by ozonation during flushing with micro-nano-bubble solution, Journal of Contaminant Hydrology 202 (2017) 1–10.

[27] N. Suwartha, D. Syamzida, C.R. Priadi, S.S. Moersidik, F. Ali, Effect of size variation on microbubble mass transfer coefficient in flotation and aeration processes, Heliyon 6 (4) (2020) e03748, https://doi.org/10.1016/j.heliyon.2020.e03748.

[28] M. Takahashi, K. Chiba, P. Li, Free-Radical Generation from Collapsing Microbubbles in the Absence of a Dynamic Stimulus, The Journal of Physical Chemistry B 111 (6) (2007) 1343–1347.

[29] M. Takahashi, Y. Shirai, S. Sugawa, Free-Radical Generation from Bulk Nanobubbles in Aqueous Electrolyte Solutions: ESR Spin-Trap Observation of Microbubble-Treated Water, Langmuir 37 (16) (2021) 5005–5011.

[30] T. Temesgen, T.T. Bui, M. Han, T.-i. Kim, H. Park, Micro and nanobubble technologies as a new horizon for water-treatment techniques: A review, Advances in Colloid and Interface Science 246 (2017) 40–51.

[31] X. Wan, L.i. Zhang, Z. Sun, W. Yu, H. Xie, Treatment of High Concentration Acid Plasticizer Wastewater by Ozone Microbubble Oxidation, Water, Air, & Soil Pollution 231 (7) (2020), https://doi.org/10.1007/s11270-020-04735-3.

[32] H. Wang, Y. Wang, Z. Lou, N. Zhu, H. Yuan, The degradation processes of refractory substances in nanofiltration concentrated leachate using micro-ozonation, Waste Management 69 (2017) 274–280.

[33] T.Y. Wu, N. Guo, C.Y. The, J.X.W. Hay, Theory and Fundamentals of Ultrasound. Advances in Ultrasound Technology for Environmental Remediation, Springer Briefs in Molecular Science. Springer, Dordrecht, 2013.

[34] C. Wu, P. Li, S. Xia, S. Wang, Y. Wang, J. Hu, Z. Liu, S. Yu, The role of interface in microbubble ozonation of aromatic compounds, Chemosphere 220 (2019) 1067–1074.

[35] X. Yang, Z.e. Liu, D. Manhaeghe, Y. Yang, J. Hogie, K. Demeestere, S.W.H. Van Hulle, Intensified ozonation in packed bubble columns for water treatment: Focus on mass transfer and humic acids removal, Chemosphere 283 (2021) 131217, https://doi.org/10.1016/j.chemosphere.2021.131217.

[36] K. Yao, Y. Chi, F. Wang, J. Yan, M. Ni, K. Cen, The effect of microbubbles on gas-liquid mass transfer coefficient and degradation rate of COD in wastewater treatment, Water Science and Technology 73 (8) (2016) 1969–1977.

[37] K. Yasui, T. Tuziuti, W. Kanematsu, Mechanism of OH radical production from ozone bubbles in water after stopping cavitation, Ultrasonics Sonochemistry 58 (2019) 104707, https://doi.org/10.1016/j.ultsonch.2019.104707.

[38] J. Zhang, G.-Q. Huang, C. Liu, R.-N. Zhang, X.-X. Chen, L. Zhang, Synergistic effect of microbubbles and activated carbon on the ozonation treatment of synthetic dyeing wastewater, Separation and Purification Technology 201 (2018) 10–18.

[39] T. Zheng, T. Zhang, Q. Wang, Y. Tian, Z. Shi, N. Smale, B. Xu, Advanced treatment of acrylic fiber manufacturing wastewater with a combined microbubble-ozonation/ultraviolet irradiation process, RSC Advances 5 (95) (2015) 77601–77609.

Are microbubbles magic or just small? a direct comparison of hydroxyl radical generation between microbubble and conventional bubble ozonation under typical operational conditions

John, Alexander

2022-01-24

John A, Carra I, Jefferson B, et al., (2022) Are microbubbles magic or just small? A direct comparison of hydroxyl radical generation between microbubble and conventional bubble ozonation under typical operational conditions. Chemical Engineering Journal, Volume 435, Part 1, May 2022, Article number 134854

https://doi.org/10.1016/j.cej.2022.134854